

Supporting Information

Tailoring Carbon-Encapsulated Gold Nanoclusters via Microchip Laser Ablation in Polystyrene Solution: Controlling Size, Structure, and Photoluminescent Properties

Barana Sandakelum Hettiarachchi,^a Yumi Yakiyama^{*a,b,c} and Hidehiro Sakurai^{*a,b}

^a*Division of Applied Chemistry, Graduate School of Engineering, Osaka University, 2-1 Yamadaoka, Suita, Osaka 565-0871, Japan. E-mail: yakiyama@chem.eng.osaka-u.ac.jp, hsakurai@chem.eng.osaka-u.ac.jp*

^b*Innovative Catalysis Science Division, Institute for Open and Transdisciplinary Research Initiatives (ICS-OTRI), Osaka University, 2-1 Yamadaoka, Suita, Osaka 565-0871, Japan.*

^c*PRESTO, Japan Science and Technology Agency (JST), Kawaguchi, Saitama 332-0012, Japan.*

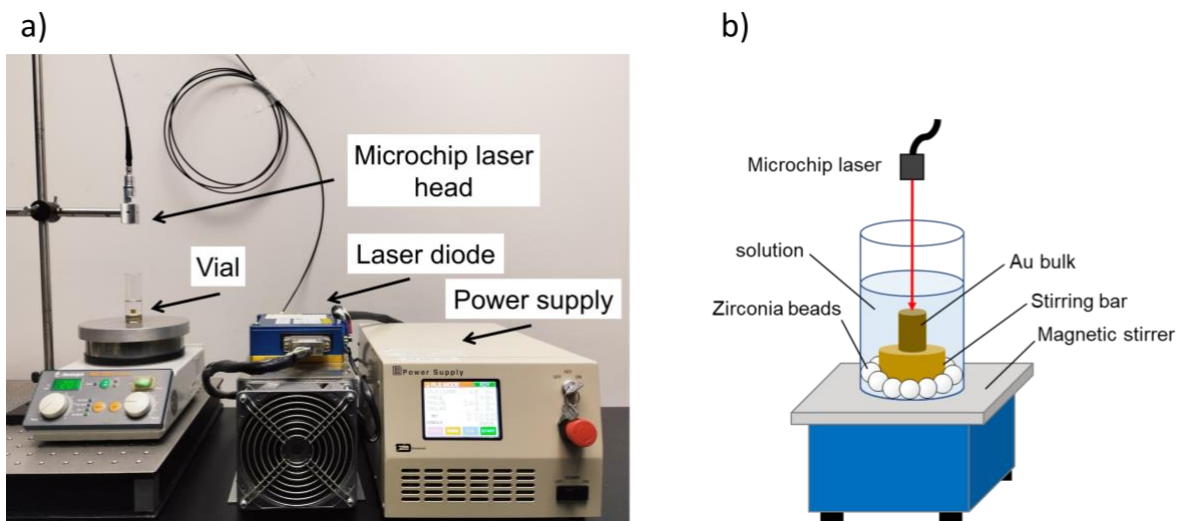


Figure S1. (a) Component of the MCL system and (b) schematic representation of the PLAL of Au using an MCL system.

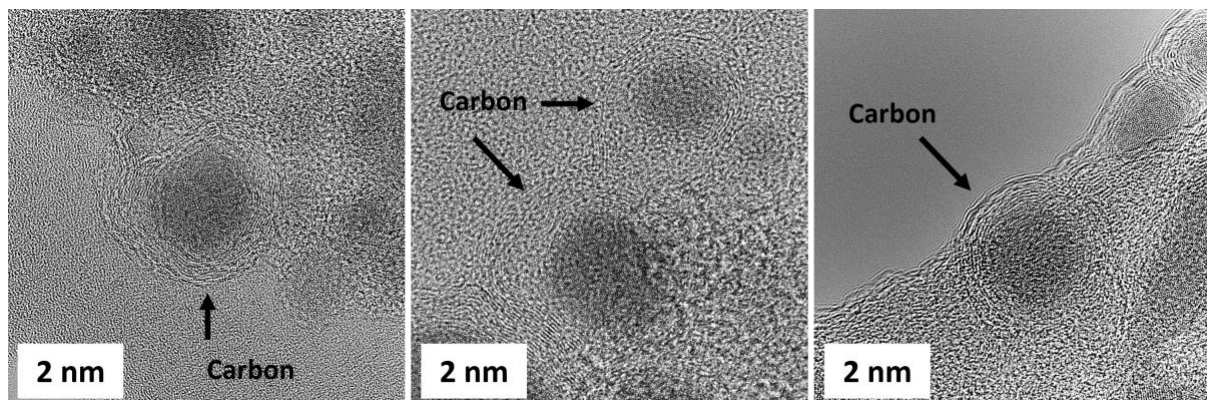


Figure S2. HRTEM image of carbon-encapsulated Au NCs prepared with 104 mW laser power in the presence of 400 mM polystyrene.

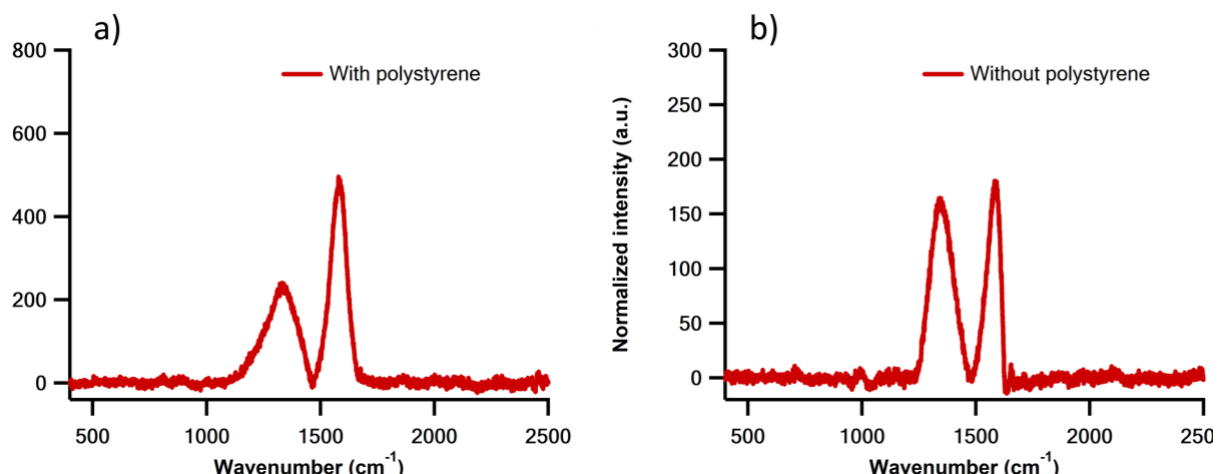


Figure S3. Raman spectrum of the carbon-encapsulated Au NCs (a) in the presence (400 mM) and (b) absence of polystyrene, respectively. Applied laser power was 104 mW.

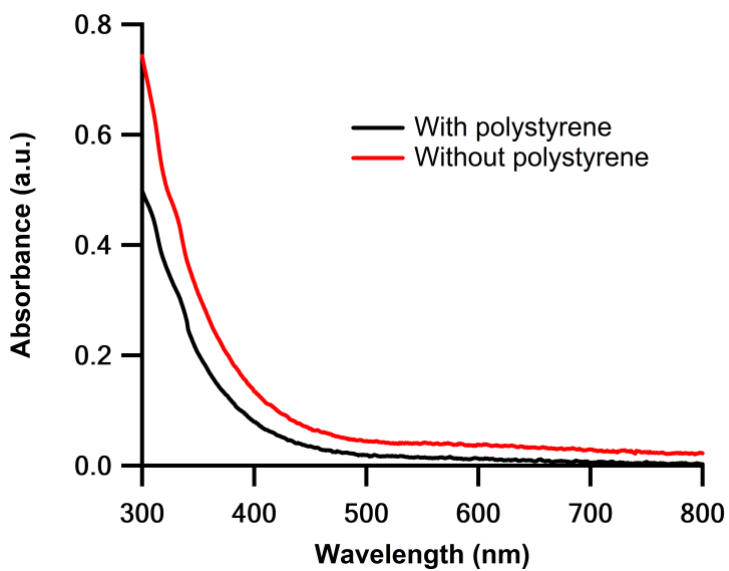


Figure S4. UV-Vis spectrum of carbon-encapsulated Au NCs in the presence (50 mM) and absence of polystyrene. The average laser power was fixed to 180 mW.

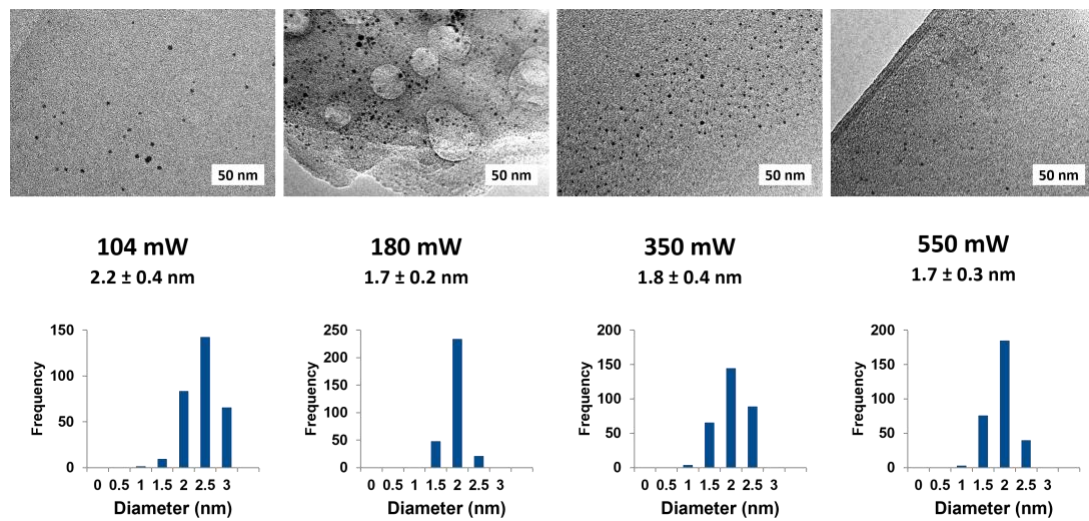


Figure S5. TEM image of carbon-encapsulated Au NCs prepared under various laser power in 50 mM polystyrene/toluene solution.

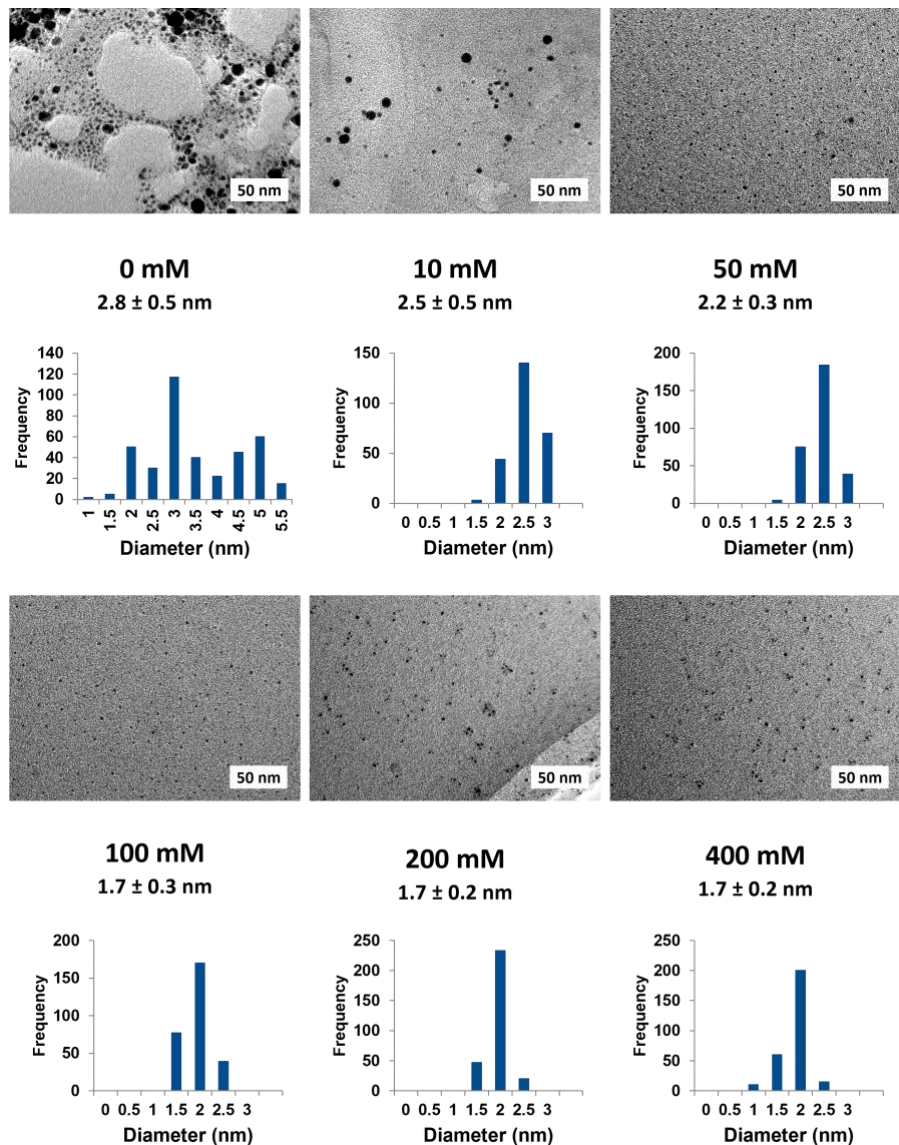


Figure S6. TEM image of carbon-encapsulated Au NCs prepared under different polystyrene concentration. Average laser power was fixed to 104 mW.

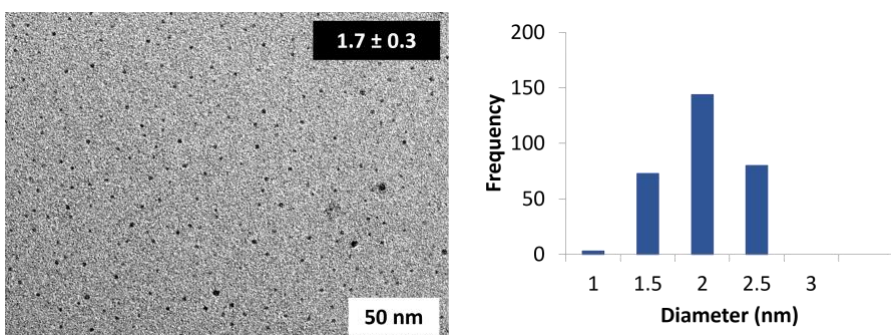


Figure S7. TEM image of carbon-encapsulated Au NCs prepared using Quanta-Ray PRO-250 laser in the presence of polystyrene (400 mM).

Carbon Layer Thickness Determination

The carbon shell thickness of the Au NCs in Table 1 and 2 was determined through extended Mie Theory fitting for core-shell type materials, which was applied to the UV-VIS spectra data in Fig. 4. Spectrum fitting was performed by using MATLAB.

Formula for Mie Theory calculations

To account for the influence of the carbon matrix on the gold particles, we utilized the extinction cross-section (σ_{ext}) for core-shell spheres. σ_{ext} is the sum of the absorption cross-section (σ_{abs}) and the scattering cross-section (σ_{sca}):

$$\sigma_{ext} = \sigma_{abs} + \sigma_{sca} \quad (1)$$

For particles much smaller than the wavelength of light, the scattering contribution (σ_{sca}) becomes negligible due to its R^6 dependence.^{S1} Thus, simulated extinction cross-section mainly reflects absorption phenomena similar to the observed experimental UV-Vis spectrum. The extinction coefficient, $\sigma_{ext}(\omega)$, is given by:

$$\sigma_{ext}(\omega) = 4\pi k \operatorname{Im}[\alpha(\omega)] \quad (2)$$

where k is the wavenumber of the electromagnetic radiation, and $\operatorname{Im}[\alpha(\omega)]$ is the imaginary part of the polarizability.^{S2} In the quasi-static regime, the following dipolar approximation for the polarizability ($\alpha(\omega)$) of the core-shell sphere is applies:

$$\alpha(\omega) = \frac{4\pi}{3} (R + d)^3 \epsilon_0 \frac{(\epsilon_{shell} - \epsilon_m)(\epsilon_{core} + 2\epsilon_{shell}) + (\frac{R}{R+d})^3 (\epsilon_{core} - \epsilon_{shell})(\epsilon_m + 2\epsilon_{shell})}{(\epsilon_{shell} + 2\epsilon_m)(\epsilon_{core} + 2\epsilon_{shell}) + (\frac{R}{R+d})^3 (\epsilon_{core} - \epsilon_{shell})(2\epsilon_{shell} - \epsilon_m)} \quad (3)$$

where R is the Au NC core radius, d is the carbon shell thickness, ϵ_0 is the vacuum permittivity, ϵ_{shell} is the dielectric function of the carbon shell, ϵ_{core} is the dielectric function of the Au NC core.^{S1,S3} ϵ_m is the dielectric function of the surrounding medium (2.2) (here toluene).^{S4}

The bulk dielectric function for a metal is given by the Drude model by introducing of (ϵ_0) interband transitions to the polarizability:

$$\epsilon(\omega, R) = \epsilon_0 - \frac{\omega_p^2}{\omega^2 + i\omega\Gamma(R)} \quad (4)$$

where ω_p is the plasma frequency of gold (9 eV).^{S5} $\Gamma(R)$ accounts for size-dependent relaxation, modeled as:

$$\Gamma(R) = \Gamma_\infty + \frac{AV_F}{R} \quad (5)$$

where V_F is the Fermi velocity of electrons in Au (1.4×10^6 m/s).^{S1,S5} Γ_∞ is the bulk metal's relaxation constant (0.07 eV).^{S5} A is a constant with a value near 1. R is the radius of the Au NC. Thus equation 3 will be represented as follows.^{S5}

$$\epsilon(\omega, R) = \epsilon_0 - \frac{\omega_p^2}{\omega^2 + i\omega(\Gamma_\infty + \frac{AV_F}{R})} \quad (6)$$

The size-dependent dielectric function can be split into real and imaginary parts as eq. (7).^{S1}

$$\epsilon(\omega, R) = \epsilon_1(\omega) + i\epsilon_2(\omega) \quad (7)$$

$\epsilon_1(\omega)$ and $\epsilon_2(\omega)$ are real and imaginary parts represented as eq. (8) and (9), respectively.^{S6}

$$\epsilon_1(\omega, R) = \epsilon_0 - \frac{\omega_p^2 \Gamma(R)^2}{1 + \omega^2 \Gamma(R)^2} \quad (8)$$

$$i\epsilon_2(\omega, R) = \frac{\omega_p^2 \Gamma(R)}{\omega(1 + \omega^2 \Gamma(R)^2)} \quad (9)$$

The full size-dependent dielectric function, combining real and imaginary parts, is:

$$\epsilon(\omega, R) = \left[\epsilon_{1\infty}(\omega) + \frac{\omega_p^2}{\omega^2 + \Gamma_\infty^2} - \frac{\omega_p^2}{\omega^2 + \Gamma(R)^2} \right] + i \left[\epsilon_{2\infty}(\omega) + \frac{\omega_p^2 \Gamma(R)}{\omega(\omega^2 + \Gamma(R)^2)} - \frac{\omega_p^2 \Gamma_\infty}{\omega(\omega^2 + \Gamma_\infty^2)} \right] \quad (10)$$

where $\epsilon_{1\infty}(\omega)$ and $\epsilon_{2\infty}(\omega)$ are the real and imaginary components of the bulk dielectric function of Au.^{S1}

Table S1. Adjusted fitting parameters for the UV-Vis spectrum of carbon-encapsulated Au NCs under different laser powers

	ϵ_s^a		$(\Gamma(R)^b \times 10^{15}$ (rad/s)	$\epsilon(\omega, R)^c$							
	300			400		500		600			
Laser power (mW)	Re	Im		Re	Im	Re	Im	Re	Im	Re	Im
104	-0.5	3	1.65	-1.1	2.7	-0.8	3	-0.6	2.6	-0.4	2.4
180	-0.7	3.3	1.75	-1.25	3.1	-0.9	3.3	-0.6	3	-0.3	2.8
350	-0.8	3.4	1.7	-1.3	3.2	-0.9	3.4	-0.6	3.1	-0.4	2.9
550	-0.85	3.6	1.8	-1.4	3.4	-1	3.6	-0.7	3.2	-0.4	3

a. Dielectric function of carbon shell.

b. Size-dependent relaxation constant.

c. Wavelength-dependent dielectric function of gold at key wavelengths.

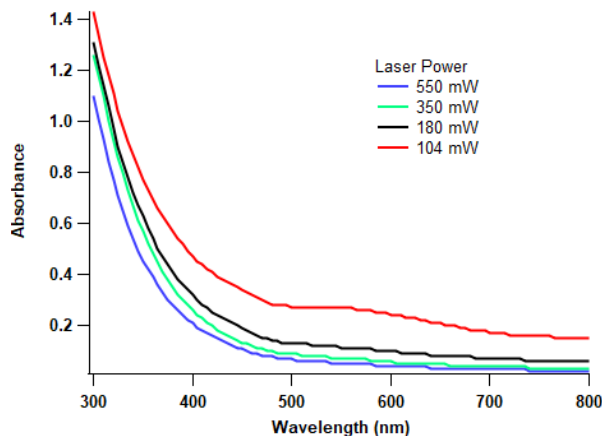


Figure S8. Simulated UV-Vis spectrum of carbon-encapsulated Au NCs under different laser powers.

Table S2. Adjusted fitting parameters for the UV-Vis spectrum of carbon-encapsulated Au NPs under different polystyrene concentration

	ϵ_s^a		$(\Gamma(R)^b \times 10^{15}$ (rad/s)	$\epsilon(\omega, R)^c$								
				300		400		500		600		
Polystyrene concentration (mW)	Re	Im	Re	Im	Re	Im	Re	Im	Re	Im	Re	Im
0	-0.7	3.3	1.5	-1.4	3.1	-1	3.3	-0.8	3	-0.5	2.8	
10	-0.7	3.3	1.6	-1.2	3.2	-0.9	3	-0.6	2.8	-0.4	2.6	
50	-0.5	2.8	1.72	-1.2	2.8	-0.8	3	-0.5	2.7	-0.3	2.5	
100	-0.5	3	1.8	-1.2	2.8	-0.8	3	-0.5	2.7	-0.3	2.5	
200	-0.4	2.7	1.8	-1.2	2.7	-0.8	2.9	-0.5	2.5	-0.3	2.4	
400	-0.4	2.7	1.8	-1.2	2.6	-0.8	2.8	-0.5	2.5	-0.2	2.3	

a. Dielectric function of carbon shell.

b. Size-dependent relaxation constant.

c. Wavelength-dependent dielectric function of gold at key wavelengths.

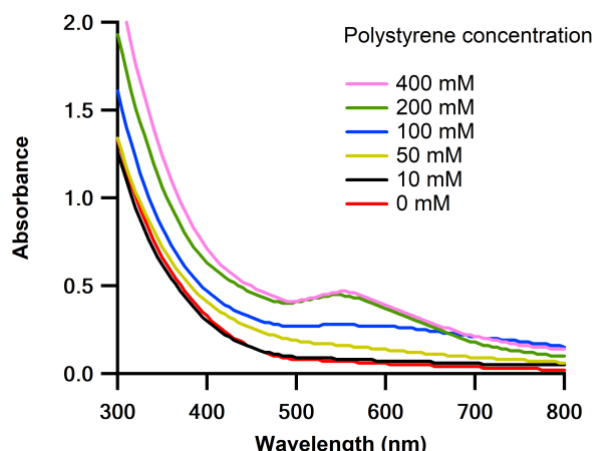


Figure S9. Simulated UV-Vis spectrum of carbon-encapsulated Au NCs under different polystyrene concentrations.

References

- 1 U. Kreibig, M. Vollmer, Optical Properties of Metal Clusters; Springer-Verlag: Berlin, 1995.
- 2 I. Sersic, C. Tuambilangana, T. Kampfrath, A. F. Koenderink, Magneto-electric point scattering theory for metamaterial scatterers. *Phys. Rev. B*, 2011, **83**, 245102.
- 3 V. Amendola, G. A. Rizzi, S. Polizzi, M. Meneghetti, Synthesis of gold nanoparticles by laser ablation in toluene: quenching and recovery of the surface plasmon absorption. *J. Phys. Chem. B*, 2005, **109**, 23125-23128.
- 4 C. Rønne, K. Jensby, B. J. Loughnane, J. Fourkas, O. F. Nielsen, S. R. Keiding, Temperature dependence of the dielectric function of $C_6H_6(l)$ and $C_6H_5CH_3(l)$ measured with THz spectroscopy. *J. Chem. Phys.* 2000, **113**, 3749-3756.
- 5 A. Derkachova, K. Kolwas, I. Demchenko, Dielectric Function for Gold in Plasmonics Applications: Size Dependence of Plasmon Resonance Frequencies and Damping Rates for Nanospheres. *Plasmonics*, 2016, **11**, 941-951.
- 6 S. A. Maier, Plasmonics - Fundamentals and Applications. New York, U.S.A.: Springer, 2007.